

Mean-field theory of acentric order of dipolar chromophores in polymeric electro-optic materials

Yuriy V. Pereverzev* and Oleg V. Prezhdo

Department of Chemistry, University of Washington, Seattle, Washington 98195-1700

(Received 28 February 2000)

A mean-field theory of macroscopic order of dipolar chromophores in a polymer matrix in the presence of an external electric field is developed. The theory is applied to characterize the electro-optic coefficient of the Pockel effect that forms the basis for a variety of polymeric nonlinear electro-optic materials. The coefficient is studied as a function of chromophore concentration, polymer properties, and manufacturing conditions, including temperature, strength of the applied electric field, and macroscopic shape of the sample. The model reproduces the observed behavior of the electro-optic coefficient and explains the nonlinear concentration dependence of the coefficient at high chromophore concentrations. Specific recommendations for system design are suggested from the analysis of the obtained data.

PACS number(s): 78.30.Jw, 64.60.Cn, 77.84.Jd, 85.60.Bt

I. INTRODUCTION

Polymeric materials with macroscopic optical nonlinearities are currently achieving numerous applications [1–6]. To name just a few, electro-optic polymeric materials are used in fiber optic transmission lines and amplifiers, electrical-to-optical signal transducers for cable television, diode lasers, high-density memories, flat panel displays, and biomedical voltage sensing. The realization of the required high macroscopic electro-optical activity demands optimization of several types of properties in these materials. These properties include molecular polarizabilities of the optically active components, optical quality, and stability of the materials to thermal, mechanical, and electric fields applied during processing and operation.

The focus of this paper is on a class of optically nonlinear materials that are obtained by dissolving chromophore molecules in inert polymer matrices. The optical activity of such materials relies on the macroscopic acentric order that chromophore molecules attain in a liquid polymer that is subsequently frozen. A typical chromophore is an asymmetric quasilinear conjugated molecule that carries a large dipole moment due to the presence of electron donor and acceptor groups at the ends. Such molecules are characterized by a highly nonlinear molecular polarizability. Combined with the acentric order, the nonlinear molecular polarizability results in a macroscopic electro-optic response.

The macroscopic acentric order in the polymeric electro-optic materials can be achieved by application of a strong external electric field to a polymer with dissolved chromophore molecules. The interaction between the external poling field and the dipole moments of the molecules results in a thermodynamically preferred orientation for the chromophores. To speed up the equilibration, the poling field is applied to the sample at a temperature that is above the glass transition temperature at which the polymer becomes rubbery. Under these conditions, the solution of the chromophore molecules in the polymer rapidly acquires a consid-

erable polarization density and the desired macroscopic acentric order. The liquid solution of the chromophores in an inert polymer is then cooled down below the glass transition temperature, still in the presence of the external field. Below the glass transition temperature, the solution becomes frozen, and the external electric field is lifted. Upon freezing, the sample exists in a long-lived metastable state with a significant asymmetry in many properties. In particular, the nonlinear optical parameters of such samples are comparable and often exceed those of the known solid state optical materials.

The nonlinear optical properties of polymeric materials with the acentric order depend on a number of parameters, including magnitudes of molecular dipole moments of chromophores, molecular hyperpolarizabilities, strength of the external poling electric field, concentration of the chromophore molecules, and molecular ionization potentials [7–11]. Experimental and theoretical studies of such materials aim to analyze these factors in order to achieve optimal optical nonlinearities of the required types.

The change in the high-frequency refractive index Δn in the presence of a low-frequency or constant electric field is the relevant optical property in this study. A low-frequency electric field of small amplitude E' is applied to a sample with the acentric chromophore order. The linear change in the optical refractive index as a function of the field $\Delta n \propto rE'$ is known as the Pockel effect. It must be noted that the electric field of the Pockel effect is entirely different from the poling field that is used to achieve the acentric order. The poling field is much stronger than the Pockel field.

The coefficient r that describes the proportionality between the Pockel field and the high-frequency refractive index depends on the concentration of chromophore molecules. It is technologically easy to change the concentration and, therewith, to control and increase the nonlinear optical effect under study. Recent experiments [1–3] led to the observation that the optical coefficient r attains a maximum as a function of the concentration, and, in some cases, significantly drops at higher chromophore concentrations. Refs. [1–3] describe a theoretical approach that provides an explanation of this highly undesirable behavior of the optical coefficient. A different theoretical model is proposed in this work. The present model treats the chromophore-

*Permanent address: Institute of Low Temperature Physics, Kharkov 310164, Ukraine.

chromophore interactions in a self-consistent way and is derived from the basic electrostatic principles. The model is presented in the next section, followed by discussion of the results and conclusions.

II. THEORY

Considering only the concentration dependence, the normalized expression for the optical coefficient, also called the loading parameter [1–3], can be written as [6]

$$r = \frac{N}{N_0} \langle \mu_{0z}^3 \rangle, \quad (1)$$

where μ_{0z} is the projection of the molecule dipole $\vec{\mu}_0$ of the chromophore located at the origin ‘‘0’’ on the direction of the poling field. The concentration is defined by the number of chromophore molecules N in a unit volume of the sample. It is normalized to the reference chromophore density N_0 defined below in Eq. (5). The average $\langle (\cdots) \rangle = Tr[\rho(\cdots)]$ is calculated over the equilibrium density matrix of the system

$$\rho = Z^{-1} e^{-H/T}, \quad (2)$$

where H is the Hamiltonian of the system, T is the absolute temperature, and Z is the canonical partition function

$$Z = Tr[e^{-H/T}].$$

The authors of Refs. [1–3] point out that the observed anomalous behavior of the optical coefficient with increasing chromophore concentration is due to the intermolecular interaction between the chromophores. They considered both the dipole-dipole and London intermolecular forces. The complex many-body Hamiltonian describing the interaction and entering Eq. (2) was simplified to a one site Hamiltonian. The simplification was carried out according to the theory of Piekara [12,13], which is not self-consistent. A questionable step in the Piekara based theory of the acentric order involves substitution of the statistical mechanically averaged energy of the interaction between two molecules introduced by Piekara into a further statistical mechanical averaging by Eq. (1).

The model Hamiltonian that is used to compute the average in Eq. (1) is chosen based on the similarity of the system under study with the liquid crystalline systems. As pointed out earlier, the chromophore molecules are quasilinear and are typically represented in simulations by prolate ellipsoids [1–3]. They belong to the class of molecules that form liquid-crystals, whose properties are under active investigation. Many analytical and computational results are currently available for liquid-crystal molecules. Spherical and disklike particles are often used as idealizations of certain types of liquid-crystal molecules, see for instance, Refs. [14–16]. The results obtained for systems of spherocylinders and prolate ellipsoids that are relevant for the present study are discussed below with no attempt for a complete list of citations.

If spherocylinders and prolate ellipsoids carry no dipole moment, their macroscopic thermodynamic state is determined, in the first approximation, by the excluded volume forces, see, for example, Ref. [17]. More advanced models employ the anisotropic Gay-Berne interaction potential, e.g.,

Ref. [18]. It follows from these models that dipole-less spherocylinders and prolate ellipsoids can exist in several states, including the isotropic, nematic, smectic A and smectic B states, depending on temperature and density of molecules. The isotropic phase has no order. The nematic phase exhibits only the orientation order. In addition to the orientation order, the smectic A and B phases form planes that possess long-range position order. Inside each plane the molecules are parallel to each other and perpendicular to the plane. Smectic A is also characterized by a short-ranged in-plane order that extends over a few coordination shells. The short-ranged in-plane order develops into a stronger position order in the smectic B phase.

The excluded volume force is the dominant interaction between the dipole-less liquid-crystal molecules. The main types of the liquid crystalline phases are already formed due to the excluded volume force. The anisotropic Gay-Berne interaction potential gives further details in the structure of liquid crystals. For example, it produces the position ordered structure in the planes of nematic B [18]. Similar to the anisotropic repulsive force described by the Gay-Berne potential, the attractive dipole-dipole force is secondary to the excluded volume interaction. Thus, Ref. [19] finds by the Monte Carlo simulation that in ‘‘the system of hard spherocylinders with point dipoles . . . the liquid crystal phases are relatively insensitive to the presence of the dipoles.’’ Reference [17] presents a detailed study of the system of spherocylinders with the length (L)-diameter (D) ratio $L/D=5$. It finds that the presence of the dipole-dipole interaction between the molecules slightly shifts the transition from the isotropic to the nematic phase towards higher molecular concentrations. Reference [17] concludes that the shift to higher concentrations happens due to the dipole-dipole antiparallel correlation between pairs of molecules that decreases the effective L/D aspect ratio. Increase of the effective aspect ratio is observed in systems of molecules with terminal point dipoles interacting by the Gay-Berne potential [20]. The increase comes due to the antiparallel (or antiferroelectric) correlation between the ends of molecules. As the result, the range of stability of the nematic phase is extended to lower concentrations [20]. The antiparallel correlation of such molecules is responsible for the bilayer structure where a slight tilt in the molecular axes in the adjacent planes leads to a weak ferroelectric order [21].

Correlations between point dipoles centered inside prolate molecules are investigated in Ref. [22] in the presence of an existing nematic order. The calculated Kirkwood correlation factor shows an antiparallel correlation for molecules with longitudinal dipoles and a parallel correlation for molecules with transverse dipoles [22]. Reference [23] describes dipole-dipole correlations between molecules in isotropic and smectic B phases for the dipolar Gay-Berne interaction model. The data of Ref. [23] are directly relevant for the present model. The following correlation is observed inside the planes of smectic B in the simulation [23]. The first nearest neighbor molecules are antiparallel, the second nearest neighbors are parallel, the third nearest neighbors are antiparallel, and so on. The antiparallel arrangement is formed only between the first neighbors in the isotropic phase. The results of Ref. [23] confirm that the state of the spatially disordered

system of electric dipoles is paraelectric, while the state of the spatially well ordered system [18] is antiferroelectric.

Two conclusions that are important for the present study can be made based on the references cited above. *First*, to a very good approximation, orientation and position structure of systems of prolate molecules is formed independent of the dipolar forces. *Second*, the established spatial structure must be taken into account in investigation of the electric properties of systems of dipolar molecules. The lowest energy electrically ordered state of the dipole systems will be antiferroelectric in character.

In view of the facts established above, the present work deals with the thermodynamic average (1) by restricting attention to the dipole-dipole interaction. The electric properties of the system of dipolar molecules are considered in the presence of the nematic or smectic spatial order. Since the molecular are quasilinear, the dipole-dipole interaction will be described by the Ising Hamiltonian which forms a particularly good approximation in the presence of the spatial order

$$H_d = \frac{\mu^2}{2\varepsilon} \sum_{i \neq j} \left(1 - \frac{3r_{ijz}^2}{r_{ij}^2} \right) \frac{\mu_{iz}\mu_{jz}}{r_{ij}^3}. \quad (3)$$

Here, μ is the absolute magnitude of the molecular dipole moment of the chromophore, ε is the dielectric permittivity of the polymer solvent, \vec{r}_{ij} is the radius vector between the dipoles located in positions “ i ” and “ j .” The Ising variable μ_{iz} takes only the two values of ± 1 . To our knowledge, Ref. [8] was the first to use the Ising type of dipolar states for the calculation of the thermodynamic average (1). More recent publications [24,25] employ the Ising model in order to interpret the hierarchy of phase transitions in the smectic phase in the presence of an external electric field. In a uniform external electric field, such as the poling field, the full Hamiltonian of the systems of chromophore dipoles takes the form

$$H = H_d - \frac{E\mu}{\varepsilon} \sum_i \mu_{iz}. \quad (4)$$

The following additional simplification based on the conclusions drawn above will be made for the calculation of the average (1) with the Hamiltonian (4). In the nematic state, the chromophore molecules are located at random. It is thermodynamically rigorous to define only an average distance between the molecules. The average distance is determined by the chromophore concentration. In order to avoid an additional averaging over positions of the chromophore molecules, we assume that the molecules are distributed on a lattice. Prior to the specification of the lattice type, the chromophore density is related to the longest dimension l_0 of the (quasilinear) chromophore molecule. The reference density N_0 is defined by $N_0 = l_0^{-3}$. On the scale determined by the reference density, the true density N of the chromophores is given by

$$N = N_0 x, \quad x > 0. \quad (5)$$

For example, for the ISX molecule, $l_0 = 23 \text{ \AA}$ [3] and $N_0 = l_0^{-3} = 8.2 \cdot 10^{19} \text{ cm}^{-3}$.

In the nematic phase, $N < N_0$ implies that the average distance between the centers of the molecules is isotropic in all directions. In this case the chromophore lattice is assumed to be simple cubic with the lattice constant $a = N_0^{-1/3} x^{-1/3}$. It will be shown below that in this concentration range the chromophore system of dipole exists in the paraelectric state where the exact spatial order of chromophore molecules is of little importance. As the chromophore concentration increases, the distance between the molecules decreases. Still, as long as $N < N_0$, or, equivalently, $x < 1$, the average distance is isotropic. However, as soon as $N > N_0$ and $x > 1$, only the interchromophore distances in the plane perpendicular to the main molecular axis, denoted as the z -axis, can decrease any further. The distance between the centers of the molecules along the z -axis remains fixed at l_0 . Therefore, for high concentrations we assume that chromophore molecules are located on a simple tetrahedral lattice. The lattice constant in the z direction is $b = N_0^{-1/3}$. The lattice is square in the (x,y) plane with the lattice constant $a = N_0^{-1/3} x^{-1/2}$. Lattice approximations similar to those introduced above have been used before. For instance, Ref. [26] assumes position order inside smectic planes. The lattice approximation allows us to describe the antiferroelectric state using a finite number of sublattices.

A. Paraelectric state

Using the defined lattices we consider the self-consistent mean-field approximation for the interacting dipoles. The mean-field approximation is often used in such problems, see for instance Ref. [27]. The mean-field approach is expected to reproduce all qualitative features of the system and is valid in a wide range of system’s parameters. First, we assume that the system of dipoles exists in a paraelectric state at temperature T , chromophore concentration N , and strength of the poling field E . In this case, the Hamiltonian for an individual site is straightforwardly obtained from the total Hamiltonian (4). The Hamiltonian for the dipole located at the origin “0” takes the following simple form:

$$H = - \frac{\mu_{0z}\mu}{\varepsilon} E_{\text{eff}}, \quad (6)$$

with the effective electric field given by the sum of the four terms [28]

$$E_{\text{eff}} = E + E_d + E_L + E_b.$$

The four contributions to the effective electric field are defined as follows. E is the applied poling field. E_d is the self-consistent field experienced by the selected dipole due to all other dipoles located inside a macroscopically small sphere around the selected dipole:

$$E_d = \mu\sigma \sum_i \left(3 \frac{r_{iz}^2}{r_i^2} - 1 \right) \frac{1}{r_i^3}, \quad (7)$$

where $\sigma = \langle \mu_{0z} \rangle$ is statistically mechanically averaged with the Hamiltonian (6). E_L is the Lorentz field given by

$$E_L = \frac{4\pi}{3} N \mu \sigma = \frac{4\pi}{3} N_0 x \mu \sigma. \quad (8)$$

Finally, E_b is the depolarization field that depends on the macroscopic shape of the sample. In our case, the sample is the polymer solution of chromophores that is being poled. As a rule, the poling is carried out between two planar electrodes. For this rectangular shape of the sample, assuming that it extends far in the plane of the electrodes, the depolarization field is given by the formula

$$E_b = -4\pi N \mu \sigma = -4\pi N_0 x \mu \sigma. \quad (9)$$

We note that the Piekara model [1–3] does not consider the macroscopic shape of the polymeric sample, while the current model does. The depolarization effect depends on the boundary of the sample and normalizes the external electric poling field. The presence of depolarization introduces additional chromophore concentration dependence to the optical coefficient!

Since the dipoles of the chromophore molecules are placed in a polymer matrix, all electric fields in Eq. (6) are weakened by a factor of ϵ , the dielectric permittivity of the polymer.

The Hamiltonian (6) has a simple form, and the statistical mechanical averaging of $\sigma = \langle \mu_{0z} \rangle$ with the density matrix (2) is trivial. As the result, we obtain the following self-consistent equation for σ .

$$\sigma = \tanh \frac{\mu E_{\text{eff}}}{T}. \quad (10)$$

Note, that in the current model

$$\langle \mu_{0z}^3 \rangle = \langle \mu_{0z} \rangle = \sigma, \quad (11)$$

and, therefore, Eq. (1) takes the following form

$$r = x \sigma. \quad (12)$$

Consequently, the nonlinearity of the optical coefficient r as a function of the chromophore concentration x appears entirely through the concentration dependence of σ . We consider the two cases of $x < 1$ and $x > 1$ separately.

1. Case (a). Low and moderate chromophore concentrations, $x < 1$

At low and moderate chromophore concentrations the lattice is cubic. It is well known [28] that the mean field for the cubic lattice is zero, $E_d = 0$. Therefore, the effective field inside the sample is

$$E_{\text{eff}} = E - \frac{8\pi}{3} N_0 \mu x \sigma. \quad (13)$$

Equation (11) for the parameter σ takes the following self-consistent form

$$\sigma = \tanh \left[\left(e - \frac{2\pi}{3} \eta \sigma x \right) \frac{1}{\epsilon} \right], \quad (14)$$

$$e = \frac{\mu E}{T}, \quad \eta = \frac{4\mu^2}{Tl_0^3}.$$

Equation (14) is solved numerically for arbitrary values of the parameters. In the high temperature-low poling field limit, $\mu E_{\text{eff}} < \epsilon T$, Eq. (14) admits an approximate analytic solution

$$\sigma = \frac{e}{\epsilon} \left[1 + \frac{2\pi}{3} \frac{\eta x}{\epsilon} \right]^{-1}. \quad (15)$$

The corresponding equation for the optical coefficient r , Eq. (12), takes the following form

$$r = \frac{x}{\epsilon} \left[1 + \frac{2\pi}{3} \frac{\eta x}{\epsilon} \right]^{-1} e. \quad (16)$$

This expression determines the chromophore concentration dependence of the optical coefficient for low concentrations. The expression shows that even for the cubic lattice the self-consistent model produces a nonlinear dependence of r on x .

2. Case (b). High chromophore concentrations, $x > 1$

In the presence of a large concentration of chromophores, the sum in Eq. (7) must be calculated for the tetragonal lattice arrangement of the dipoles. Generally, the calculation for each concentration of chromophores is performed only numerically. It is not possible to obtain a simple analytic dependence of the self-consistent field E_d as a function of concentration x . Still, if we include only the nearest neighbor interactions justified by the fact that the terms in the sum (7) decrease rapidly with the distance, Eq. (7) reduces to

$$E_d = -4\mu \sigma N_0 (x^{3/2} - 1). \quad (17)$$

Numerical calculations carried out for various chromophore concentrations show that the results of Eq. (17) deviate from the exact values of field E_d , Eq. (7), by 15–20%. The self-consistent equation that determines σ can now be shown to have the form

$$\sigma = \tanh \left[\left[e - \frac{2\pi}{3} \eta \sigma x - \eta \sigma (x^{3/2} - 1) \right] \frac{1}{\epsilon} \right]. \quad (18)$$

The concentration dependence of the optical coefficient is determined by an iterative solution of Eq. (18) for σ and substitution of the result into Eq. (12). Solutions for typical values of the parameters that enter Eq. (18) are presented in Sec. III.

Similarly to Eq. (15), we can derive an approximate analytic solution to Eq. (18) for situations when $\mu E_{\text{eff}} < \epsilon T$. The result is substituted into Eq. (12) producing the following expression for the chromophore concentration dependence of the optical coefficient r that is valid for high chromophore concentrations in the high temperature-low field limit

$$r = \frac{ex}{\epsilon} \left[1 + \frac{\eta}{\epsilon} \left(x^{3/2} - 1 + \frac{2\pi}{3} x \right) \right]^{-1}. \quad (19)$$

It follows from Eq. (19) that for high chromophore concentrations, $x \gg 1$, the optical coefficient is inversely propor-

tional to the square root of the concentration, $r \sim x^{-1/2}$. This implies that the optical coefficient has a maximum as a function of the chromophore concentration, Eqs. (16) and (19). The concentration x_{\max} at which the optical coefficient attains the maximum can be found in the analytical form

$$x_{\max} = \left[2 \left(\frac{\varepsilon}{\eta} - 1 \right) \right]^{2/3}. \quad (20)$$

Since Eq. (20) is derived for $x > 1$, it follows from Eq. (20) that the maximum in the optical coefficient is present only if the condition $\eta/\varepsilon < 2/3$ is satisfied. For example, for the ISX ($\mu = 8$ Debye) chromophore at temperature $T = 350$ K imbedded into a polymer with the dielectric permittivity $\varepsilon = 3$, $\eta/\varepsilon \approx 1/7$. Therefore, the optical coefficient is maximal at the concentration $x_{\max} \approx 5.25$.

B. Antiferroelectric state

The model developed above remains valid only within the range of chromophore concentrations and thermodynamic parameters, including temperature and strength of the poling field, where the paraelectric state of the chromophore lattice is stable. As has been shown in Refs. [29] for a cubic Ising lattice of dipoles, the paraelectric phase of the Ising dipole lattice becomes unstable with increasing dipole concentration and decreasing temperature, and an antiferroelectric phase appears. In contrast to the paraelectric state, the ensemble averaged value of the dipole moment in any lattice site does not vanish in the antiferroelectric state even in the absence of the poling field. At the same time, in the absence of the poling field, the macroscopic polarization of the whole sample is zero in both para- and antiferroelectric states, since the sublattices of the antiferroelectric state are polarized in the opposite directions.

The possibility of the antiferroelectric phase transition in systems of chromophore dipoles in polymer matrices should be investigated. While the paraelectric state exists independently of the spatial order, the antiferroelectric state can be more sensitive to the spatial structure of the chromophore system. A system of chromophores in a polymer matrix is clearly more complex than the cubic Ising lattice of dipoles. Liquid properties of the chromophore-polymer system may or may not inhibit formation of the spatial order that is present in the cubic lattice and favors the electrostatic order. For example, the spatial order may appear in the directions perpendicular to polymer chains due to the short-range repulsive interactions that lead to formation of the smectic B phase in liquid crystals [17]. The antiferroelectric state has been recently discovered experimentally in dipolar smectics and is currently under active investigation by both experimental and theoretical methods [18–24]. The smectic order in the inert polymer matrix may induce spatial order among the dipolar chromophore molecules and create the antiferroelectric state within the chromophore subsystem. The results presented here are derived from the microscopic molecular model defined by the dipole-dipole Hamiltonian (4).

Since typical poling temperatures are high, on the order of 350 K, and high temperatures destabilize order, it is reasonable to assume that the systems of chromophore dipoles can undergo the antiferroelectric phase transition only at high

chromophore concentrations, $x > 1$. While the phase transition may be possible even at low chromophore concentrations, $x < 1$ and the corresponding model can be easily developed, this possibility will not be presently considered.

As before, at high concentrations, $x > 1$, chromophores are assumed to form a tetrahedral lattice. The para-to antiferroelectric second order phase transition in the tetrahedral lattice of dipoles will produce the following antiferroelectric state, corresponding to the minimum of the dipole-dipole interaction energy [30]. The order will be ferroelectric along the chains of dipoles in the z -direction. The chains will show the antiferroelectric order with respect to each other. This type of the antiferroelectric order not only corresponds to the minimum of the dipole-dipole interaction energy, but also leaves the liquid properties in the direction of polymer chains intact, where a one-dimensional flow is allowed.

Similarly to antiferromagnetics [27,31], the antiferroelectric order will be described by two self-consistent fields. The field $E_{1 \text{ eff}}$ acts on the dipoles of the first sublattice, denoted by index 1. The field $E_{2 \text{ eff}}$ acts on the dipoles in the second sublattice, denoted by index 2. The expressions for these effective electric fields are derived similarly to the expression for the effective electric field in the paraelectric state:

$$E_{1 \text{ eff}} = E - \frac{8\pi}{3} N_0 \mu \sigma x + 4\mu N_0 (\sigma_1 - \sigma_2 x^{3/2}), \quad (21)$$

$$E_{2 \text{ eff}} = E - \frac{8\pi}{3} N_0 \mu \sigma x + 4\mu N_0 (\sigma_2 - \sigma_1 x^{3/2}),$$

where

$$\sigma_1 = \langle \mu_{1z} \rangle, \quad \sigma_2 = \langle \mu_{2z} \rangle, \quad \sigma = \frac{1}{2} (\sigma_1 + \sigma_2). \quad (22)$$

The averaging in Eqs. (22) is carried out with the Hamiltonian (6) using the corresponding fields of Eq. (21). The self-consistent equations for the parameters σ_1 and σ_2 take the form

$$\sigma_1 = \tanh \left[\frac{1}{\varepsilon} \left(e - \frac{\pi}{3} \eta (\sigma_1 + \sigma_2) x + \eta (\sigma_1 - \sigma_2 x^{3/2}) \right) \right], \quad (23)$$

$$\sigma_2 = \tanh \left[\frac{1}{\varepsilon} \left(e - \frac{\pi}{3} \eta (\sigma_1 + \sigma_2) x + \eta (\sigma_2 - \sigma_1 x^{3/2}) \right) \right].$$

The system of equations (29) describes both the ordered antiferroelectric state and the paraelectric state considered above. Indeed, Eq. (18) is recovered from Eqs. (23) by setting $\sigma_1 = \sigma_2$. The trivial solution of Eqs. (23) with $\sigma_1 = \sigma_2$ can be eliminated. In the antiferroelectric state $\sigma_1 \neq \sigma_2$, and the following relationships are satisfied

$$\sigma_1 - \frac{1}{2} u - \sqrt{\left(1 + \frac{1}{4} u^2 - u \tanh^{-1} g \right)} = 0, \quad (24)$$

$$e + \eta \sigma_1 \left(1 - \frac{2\pi}{3} x - x^{3/2} \right) + \eta u \left(x^{3/2} + \frac{\pi}{3} x \right) - \frac{\varepsilon}{2} \ln \frac{1 + \sigma_1}{1 - \sigma_1} = 0,$$

where

$$u = \sigma_1 - \sigma_2, \quad g = \frac{\eta u}{\varepsilon} (1 + x^{3/2}).$$

The region of the antiferroelectric state is separated in the (x, e) plane from the region of the paraelectric state by the second-order phase transition curve. The equation for the phase transition curve is obtained from Eqs. (24) in the limit $u \rightarrow 0$

$$e = \eta \sigma \left(x^{3/2} + \frac{2\pi}{3} x - 1 \right) + \frac{\varepsilon}{2} \ln \frac{1 + \sigma}{1 - \sigma}, \quad (25)$$

$$\sigma = \sqrt{\left(1 - \frac{\varepsilon}{\eta(1 + x^{3/2})} \right)}.$$

It follows from Eq. (25) that the phase transition curve intersects the concentration axis x , but does not intersect the field axis e . The point where the concentration axis is reached is calculated for the value $e = 0$, corresponding to $\sigma = 0$. The explicit expression for the concentration at this point is

$$x = \left(\frac{\varepsilon}{\eta} - 1 \right)^{2/3}.$$

In particular, the phase transition curve starts at $x = 1$, if $\varepsilon/\eta = 2$. For the typical ISX chromophore at poling temperature $T = 350$ K and polymer dielectric constant $\varepsilon = 3$, the ratio $\varepsilon/\eta \approx 7$. The phase transition curve starts at the concentration $x \approx 6^{2/3}$. According to Eq. (25), at high chromophore concentrations a linear increase in the field e corresponds on the phase transition curve to the $x^{3/2}$ increase in the concentration x .

The density of the macroscopic asymmetry in the average $\langle \mu_{0z}^3 \rangle = \sigma$ in Eq. (12) for the optical coefficient is determined in the antiferroelectric region by $\sigma = 1/2(\sigma_1 + \sigma_2)$. The values of this parameter can be found numerically from the system of equations (24).

III. RESULTS

We apply the self-consistent field theory developed in the previous section to study the dependence of the electro-optic coefficient on the chromophore concentration and the strength of the poling field. Our theory remains valid for wide ranges of the field strength, chromophore concentration, polymer dielectric constant and molecular properties, contained in parameter η , Eq. (14). The results shown here are obtained for the fixed value of $\eta = 1/3$, chosen to approximate chromophore ISX. The ISX molecule dipole moment μ is about 8 Debye and the longest linear dimension is roughly 25 Å [1–3]. At the poling temperature $T = 350$ K, η is about 1/3, according to Eq. (14).

The plane (x, e) of the reduced chromophore concentration x and poling field e , defined in Eqs. (5) and (14), respectively, is divided into the regions of the disordered paraelectric and ordered antiferroelectric states. The expressions for the electro-optic coefficient as functions of both x and e are different for the paraelectric and antiferroelectric states. Since the experimentally interesting values of x and e cover

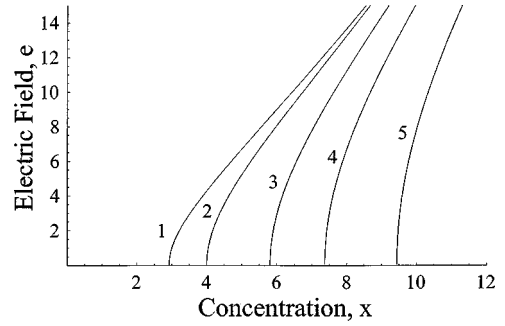


FIG. 1. Phase diagram of the macroscopic states of the chromophore lattice for different values of the polymer dielectric constant. Curves 1, 2, 3, 4, 5 correspond to the dielectric constants of 2, 3, 5, 7, and 10, respectively. The chromophore concentration x and electric field e are defined by Eqs. (5) and (14), correspondingly.

both regions, the phase transition curve separating the two regions should be found first. Figure 1 presents the phase transition curve calculated by Eq. (25) for the ISX chromophore for different values of the dielectric constant of the polymer. At low concentrations the macroscopic state of the chromophore dipoles is paraelectric. As the concentration is increased, the second-order phase transition takes place, and the macroscopic system of dipoles becomes antiferroelectric. The phase transition happens at higher concentration as the strength of the external electric poling field is increased. The presence of a strong external electric field disrupts the antiferroelectric order in the chromophore system. The disordered paraelectric state can be always achieved by destroying the antiferroelectric state with a strong poling field.

The external field-chromophore interaction dominates the interchromophore coupling in strong electric fields. The interchromophore coupling becomes more important with increasing chromophore concentration at a fixed value of the field. The dielectric constant of the polymer acts to decrease the effect of the external field and also changes the magnitude of the dipole-dipole interaction. Higher concentrations of the chromophore are required to achieve the antiferroelectric state inside polymer matrices with larger dielectric constants: The phase transition curve in Fig. 1 shifts towards higher chromophore concentrations for larger polymer dielectric constants.

When the poling field is weak and the chromophore concentration is low, the magnitude of the electro-optic coefficient grows linearly both with the chromophore concentration x and with the strength of the poling field e . In strong fields and at high chromophore concentrations significant deviations from the linear behavior are observed. Consider first the concentration dependence of the electro-optic coefficient. Figure 2 depicts the electro-optic coefficient r , Eq. (12), as a function of the concentration for different fixed values of the poling field and polymer dielectric constant. The expected behavior of the electro-optic coefficient always follows the lowest curve. Different curves in the figure correspond to different macroscopic states and different levels of approximation for the coefficient. The long-dashed curve describes the electro-optic coefficient of the antiferroelectric state. The other three curves describe the paraelectric state. The top-most short-dashed curve describes noninteracting chromophores on a cubic lattice neglecting the Lorentz and de-

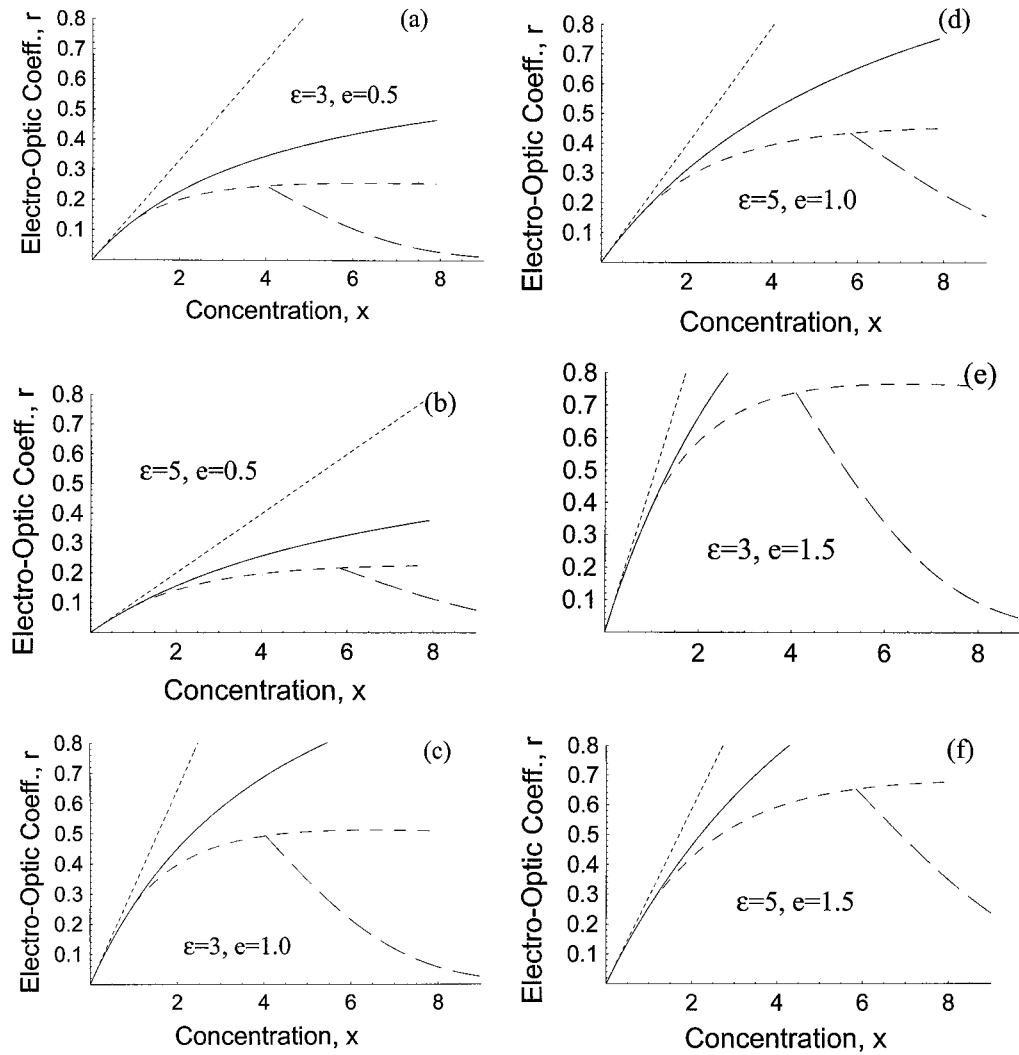


FIG. 2. Electro-optic coefficient r , Eq. (12), as a function of the chromophore concentration x , Eq. (5), for the indicated values of the polymer dielectric constant ϵ and the strength of the poling electric field e defined in Eq. (14). The middle dashed line corresponds to the paraelectric state, the long-dashed line gives the antiferroelectric state. The short dashed and solid lines are due to the simplified paraelectric state models as described in the text.

polarization fields, Eqs. (8) and (9). In this approximation, the statistical mechanically averaged value of the chromophore dipole moment does not depend on the chromophore concentration and is calculated by Eq. (10) with the effective field equal to the poling field. In this simplest of the approximations the electro-optic coefficient is always a linear function of the concentration, Eq. (12).

The solid line shows the electro-optic coefficient calculated rigorously for the paraelectric cubic lattice of dipoles including all effects, including the Lorentz and depolarization contributions to the electric field. The average value of the chromophore dipole moment depends on the effective electric field, which, in turn, depends on the average value of the chromophore dipole moment, Eq. (13). Therefore, the average value of the dipole moment has to be calculated in a self-consistent manner, Eq. (14). The interaction between the chromophore dipoles is included in the mean-field approximation. The mean-field dipole-dipole interaction vanishes on the cubic lattice due to symmetry. The solid curve describes the electro-optic coefficient at low and moderate chromophore concentrations when the distance between chro-

mophore molecules is greater than the linear dimension of each molecule. At such concentrations the shape of the molecule is irrelevant. It should be noted that even in this simplest case the electro-optic coefficient changes nonlinearly with the concentration due to the presence of the concentration dependent Lorentz and depolarization field. This effect has not been included in the earlier models [1–3]. The depolarization effect depends on the macroscopic shape of the sample and is calculated here for rectangular samples that are commonly used in experimental setups. For spherical samples, the Lorentz and depolarization fields will identically cancel and the linear dependence given by the short-dashed line will be recovered. As evidenced by the results in Figs. 2, the electro-optic coefficient can strongly depend on the macroscopic shape of the sample.

At high chromophore concentrations when the average distance between the chromophore molecules is less than the longest dimension of each molecule, the chromophore dipoles can no longer be placed on a cubic lattice. Since chromophore molecules are typically long and narrow [1–3], at high concentrations they must remain a fixed distance apart

in the longest dimension and can approach each other in the other two dimensions. This arrangement leads to the tetrahedral lattice. The mean field experienced by a selected dipole due to all other dipoles around it does not vanish for the tetrahedral lattice, Eq. (17), and contributes to the effective electric field. The statistically mechanically averaged value of the chromophore dipole is now calculated by Eq. (17). Plugged into Eq. (12) for r , it produces the dashed curves in Figs. 2. The dashed curves exhibit maxima, whose locations are determined by Eq. (20). The experimental data for the ISX chromophore system [1–3] are best described by this model (see discussion of Fig. 4 below).

Liquid crystal-like order of chromophores [17] will favor the antiferroelectric state [18–24] that can become more stable than the paraelectric state of the dipoles as chromophore concentration is increased. The chromophore system may undergo a second order phase transition. The critical concentration where the transition takes place is determined by the phase transition curve, Eq. (25), Fig. 1. Our mean-field model describes the antiferroelectric state on the microscopic level by two interacting sublattices, each with its own effective electric field and average value of the chromophore dipole moment, Eqs. (21). The average dipole moment of the total system is given by the sum of the dipole moments in each sublattice, Eq. (22). The dipole moments in the sublattices are calculated self-consistently by Eqs. (23). The resulting electro-optic coefficient, Eq. (12), is plotted in Figs. 2 by the long-dashed lines and gives the lowest of the four curves. The electro-optic coefficient suffers a sharp decline due to the para- to antiferroelectric phase transition.

As the strength of the poling field increases for the same chromophore-polymer system, Figs. 2(a), 2(c), and 2(e) and 2(b), 2(d), and 2(f) the electro-optic coefficient becomes larger. At the same time, the maximum value of the coefficient is shifted slightly to higher chromophore concentrations. If the strength of the poling field is kept the same, while the dielectric constant of the polymer matrix is increased, Figs. 2(a) and 2(b), 2(c) and 2(d), and 2(e) and 2(f), the effective field inside the polymer matrix felt by the chromophore becomes smaller. As the result, the electro-optic coefficient decreases, although the maximum is noticeably shifted to higher concentrations. While stronger poling fields always produce larger electro-optic coefficients, the effect of the dielectric constant of the polymer matrix is twofold. Generally, smaller dielectric constants are better, since they lead to larger effective poling fields inside the sample. Nevertheless, at high chromophore concentrations, too low a value of the dielectric constant may result in the undesirable phase transition. Optimal values of the dielectric constant of the polymer matrix should be selected to avoid the phase transition and, at the same time, to maximize the effective field inside the sample.

It is instructive to consider the electro-optic coefficient at fixed chromophore concentrations as a function of the poling field, Figs. 3. The four curves representing the four models remain the same as before. While in Figs. 2 the differences between the models are apparent at high values of the abscissa, the differences appear at low values of the abscissa in Figs. 3. Strong electric fields saturate the electro-optic coefficient independent of the approximation. The four models differ only for weak poling fields. As in Figs. 2, the expected

behavior of the electro-optic coefficient including all effects follows the lowest curve. The simpler models overestimate the value of the coefficient at low fields.

Figures 3(a), 3(b), and 3(d) show three data curves, while Figs. 3(c), 3(e), and 3(f) show four. The fourth curve describing the antiferroelectric state is absent in Figs. 3(a), 3(b), and 3(d) since the para- to antiferroelectric phase transition can not take place at the chosen values for the chromophore concentration and the polymer matrix dielectric constant, according to the phase transition line, Fig. 1. Figures 3(c), 3(e), and 3(f) do show the antiferroelectric curve. The antiferroelectric curve is qualitatively different from all three paraelectric curves. This difference can be studied analytically for high concentrations and low electric fields. The average value of the dipole moment σ is proportional to the field e in the paraelectric state. The proportionality coefficient is a power function of the concentration x , as follows from Eq. (19). In the ordered antiferroelectric state only the sum $\sigma_1 + \sigma_2$ and not the individual average dipole moments of the two sublattices σ_1 and σ_2 is directly proportional to the field e . Taking into account that the absolute magnitudes of the individual values of σ_1 and σ_2 are close to unit, it follows from Eq. (23) that $\sigma_1 + \sigma_2 \propto e \cdot \exp(-2\eta x^{3/2}/\epsilon)$. The proportionality coefficient is now an exponential function of the chromophore concentration x , in contrast to the paraelectric state, where the coefficient was a power of x . The differences in the concentration dependence of the average dipole moments in the para- and antiferroelectric states lead to the differences in the electro-optic coefficients. These low field results are best reflected in Fig. 3(e).

Next, compare the experimental [1–3] and theoretical data for the concentration dependence of the electro-optic coefficient (loading parameter) of the ISX chromophore system, Fig. 4. The accurate values of the variables of our model for the ISX system of Refs. [1–3] are $\eta=0.409$, $e=1.56$, and $\epsilon=2.5$. The data are presented in Fig. 4 and are normalized to the maximum value of the electro-optic coefficient. The experimental data are given by the solid circles. The theoretical curves in Fig. 4 correspond to the same approximations as before in Figs. 2 and 3. In contrast to Figs. 2 and 3, the concentration is now given by the number density of the chromophore molecules as in Refs. [1–3]. Comparing the experimental and theoretical data we conclude that the system of chromophores in the chosen polymer matrix [1–3] remains in the paraelectric state even at high chromophore concentrations. In the region of concentrations where formation of the antiferroelectric state becomes possible according to our model 4, Sec. II B, the phase transition does not take place experimentally. It is likely that liquidlike behavior of the polymer matrix dominates preventing formation of the ordered state. It is also possible that on the time scale of the experiment the paraelectric state remains metastable and does not convert to the antiferroelectric state. Similar to the experimental data, the theoretical curve describing the paraelectric state at high chromophore concentrations goes through a maximum as discussed at the end of Sec. II A. At high chromophore concentrations the experimental data lie below the paraelectric curve, indicating that the dipole-dipole interaction is stronger than predicted by the mean-field model. Extensions of the mean-field approximation that incorporate dipole-dipole correlation effects are expected to

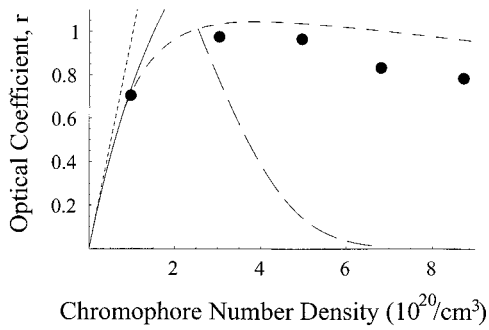


FIG. 4. Normalized electro-optic coefficient r as a function of the chromophore number density for the ISX chromophore system of Refs. [1–3]. The notation is the same as in Fig. 2. Circles indicate experimental data.

improve the agreement between the experimental and theoretical data for the concentration dependence of the electro-optic coefficient in the paraelectric state.

IV. CONCLUSIONS

The paper presents the first self-consistent mean-field model for the acentric order of dipolar chromophores in

polymeric electro-optic materials. The model correctly describes all qualitative features of the electro-optic coefficient observed in the experimental data and produces good quantitative agreement with the experimental data for a typical electro-optical system. The model is fully self-consistent, is derived from the basic electrostatic principles and contains no adjustable parameters.

The properties of the electro-optic coefficient are determined by the interplay of the chromophore-poling field and chromophore-chromophore interactions. At low chromophore concentrations, the chromophore-poling field interaction dominates. At high chromophore concentrations, the chromophore-chromophore coupling becomes very important, while the effect of the poling field markedly depends on its strength.

Maximization of the electro-optic coefficient is the primary goal in the materials design. The experimentally observed maximum in the electro-optic coefficient and its subsequent decrease with increasing chromophore concentration are shown to be due to both excluded volume and electrostatic interactions between the chromophore molecules. The excluded volume constraints originate from the short-ranged repulsive forces between molecules and determine the spatial

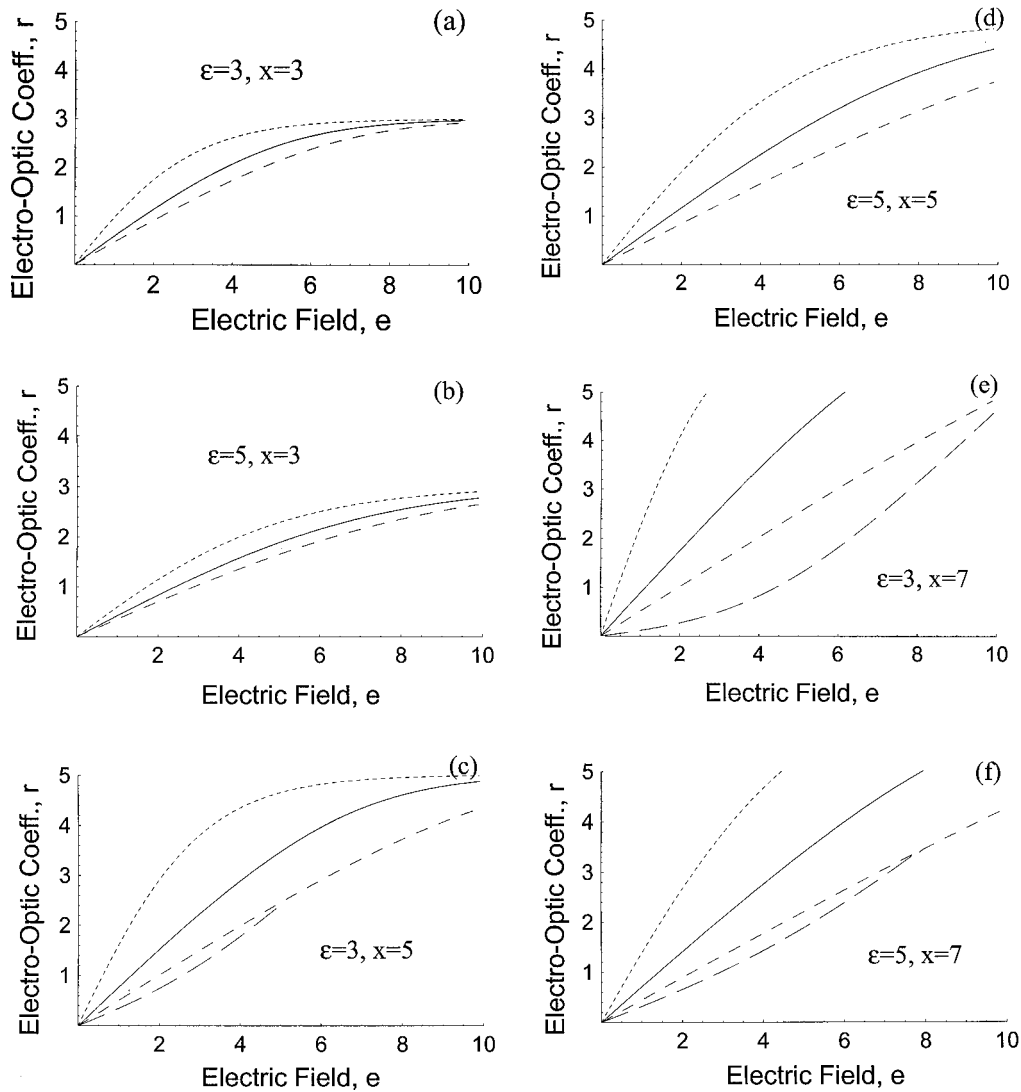


FIG. 3. Electro-optic coefficient r , Eq. (12), as a function of the strength of the poling electric field e , Eq. (14), for the indicated values of the polymer dielectric constant ϵ and chromophore concentration x defined in Eq. (5). The notation is the same as in Fig. 2.

arrangement of chromophores. The long-ranged Coulomb interaction between the chromophore dipoles controls the macroscopic polarization.

The model developed here predicts that stronger poling fields are always preferred. Smaller values of the dielectric constant of the polymer matrix are generally better, since the effective poling field inside the sample is increased with a decreasing dielectric constant. Nevertheless, at high chromophore concentrations, a low value of the dielectric constant may result in the para- to antiferroelectric phase transition, leading to a dramatic decrease of the electro-optic coefficient. Therefore, at high chromophore concentrations, an optimization of the polymer dielectric constant may be needed, so as to avoid the phase transition, while maximizing the effective poling field inside the sample. For any chromophore concentration, a sufficiently large poling field destroys the antiferroelectric phase preserving the paraelectric phase. Lack of spatial order in the system of chromophore dipoles should also favor the paraelectric state.

The current model predicts that the electro-optic coefficient may significantly depend on the macroscopic shape of the sample used in the poling process. The spherical shape is most favorable, provided that all other poling conditions remain fixed. At high chromophore concentrations significant loss of electro-optic properties can be observed for rectangular shaped samples. The effect of the macroscopic shape of the sample on the effective poling field inside the sample can be easily exploited in experimental designs.

The experimental data for one typical material considered here are best described by the paraelectric model. The observed differences between the experimental and theoretical data are due to various approximations involved in our models. The following are the important ones. First, the chromophore-chromophore interactions are treated within the self-consistent mean-field approach. Dipole-dipole correlation effects increase the role of the interchromophore coupling and are expected to bring the theoretical curve in closer agreement with the experimental data. Approximate treatment of the correlation effects within the present model will be investigated further in a subsequent publication. Even on the mean-field level, our model gives a reliable description of the observed phenomenon.

The system of chromophores with interacting dipoles is considered on a lattice, discounting the possibility of liquid-like behavior of chromophore molecules in a polymer matrix. Liquid properties result in fluctuations and disorder in positions of the molecules. We emphasize that the lattice

approximation is by no means critical for the properties of the paraelectric state of the dipole system. The lattice approximation simplifies the calculation of the macroscopic polarization allowing us to obtain analytic results. Numerical solution of the problem without the lattice approximation will lead to similar results for the paraelectric phase. On the other hand, the presence of a spatial lattice appears important for observation of the antiferroelectric state. The lattice approximation is justifiable by the possibility of the liquid-crystal behavior of the polymer under the poling conditions. The structure obtained during poling is preserved at later times by freezing the polymer below the glass transition temperature. The lattice approximation is also justifiable by the system design, in particular, in the systems where the chromophore molecules are equally spaced by direct chemical attachment to polymer chains. While the antiferroelectric state negatively affects the electro-optic coefficient and is not observed for the ISX chromophore system, its presence is an interesting physical phenomenon by itself. It is expected that the antiferroelectric state can be found, for example, in systems of chromophores dissolved in liquid crystalline polymers.

The point dipole model of the chromophores constitutes another important approximation in the description of the interchromophore interaction. This approximation is valid at low chromophore concentrations, but should break down if the chromophore concentration is sufficiently high. The dipole approximation works quite well for high chromophore concentrations, since the dipole-dipole Hamiltonian reflects the main contribution to the interaction energy even when the chromophore molecules are close to each other. Explicit consideration of charge distributions within the chromophore molecules can improve the agreement with the experiment and will be considered. Polarization of each molecule in the presence of the poling field and chromophore-chromophore coupling is yet another avenue for improvement. As it is, the present model in closed analytic form reflects the key features of the problem and provides good quantitative agreement with the experimental data.

ACKNOWLEDGMENTS

The authors are grateful to Larry Dalton and Bruce Robinson for illuminating discussions of the problem under study and for the experimental data set for the ISX system. Financial support from the Camille and Henry Dreyfus Foundation and Research Corporation are gratefully acknowledged.

-
- [1] A. W. Harper, S. Sun, L. R. Dalton, S. M. Garner, A. Chen, S. Kalluri, W. H. Steier, and B. H. Robinson, *J. Opt. Soc. Am. B* **15**, 329 (1998).
- [2] B. H. Robinson, L. P. Dalton, A. W. Harper, A. Ren, F. Wang, C. Zhang, G. Todorova, M. Lee, R. Aniszfeld, S. Garner, A. Chen, W. H. Steier, S. Houbrecht, A. Persoons, I. Ledoux, J. Zyss, and A. K. Y. Jen, *Chem. Phys.* **245**, 35 (1999).
- [3] A. K. Y. Jen, Y. Q. Liu, L. X. Zheng, S. Liu, K. Y. Drost, Y. Zhang, and L. R. Dalton, *Adv. Mater.* **11**, 452 (1999).
- [4] I. G. Voigt-Martin, G. Li, U. Kolb, H. Kothe, A. V. Yakimanski, A. V. Tenkovtsev, and C. Gilmore, *Phys. Rev. B* **59**, 6722 (1999).
- [5] L. C. D. Romero and D. L. Andrews, *J. Phys. B* **32**, 2277 (1999).
- [6] J. Zyss and J. L. Oudar, *Phys. Rev. A* **26**, 2028 (1982).
- [7] D. J. Williams, ed., *Nonlinear Optical Properties of Organic and Polymeric Materials*, ACS Symp. Ser. 233 (American Chemical Society, Washington, D.C., 1983).
- [8] G. R. Meredith, J. G. van Dusen, and D. J. Williams, *Macromolecules* **15**, 1385 (1982).

- [9] K. D. Singer, M. G. Kuzuk, and J. E. Sohn, *J. Opt. Soc. Am. B* **4**, 968 (1987).
- [10] C. P. Van der Vorst and S. J. Pihen, *Proc. SPIE* **99**, 866 (1987).
- [11] C. P. Van der Vorst and S. J. Pihen, *J. Opt. Soc. Am. B* **7**, 320 (1990).
- [12] A. Piekara, *Z. Phys.* **108**, 395 (1938).
- [13] A. Piekara, *Proc. R. Soc. London, Ser. A* **172**, 360 (1939).
- [14] D. Wei and G. N. Patey, *Phys. Rev. Lett.* **68**, 2043 (1992).
- [15] G. Auton and G. N. Patey, *Phys. Rev. Lett.* **76**, 239 (1996).
- [16] G. Auton, D. Q. Wei, and G. N. Patey, *Phys. Rev. E* **55**, 447 (1997).
- [17] S. C. McGrother, A. Gil-Villegas, and G. Jackson, *Mol. Phys.* **95**, 657 (1998).
- [18] M. A. Bates and G. R. Luckhurst, *J. Chem. Phys.* **110**, 7087 (1999).
- [19] D. Levesque, J. J. Weis, and G. J. Zarragoicoechea, *Phys. Rev. E* **47**, 496 (1993).
- [20] K. Saton, S. Mita, and S. Kondo, *Chem. Phys. Lett.* **255**, 99 (1996).
- [21] R. Berardi, S. Orlandi, and C. Zannoni, *Chem. Phys. Lett.* **261**, 357 (1996).
- [22] D. A. Dunmur and P. Palfy-Muhoray, *Mol. Phys.* **76**, 1015 (1992).
- [23] M. Houssa, A. Oulid, and L. F. Rull, *Mol. Phys.* **94**, 439 (1998).
- [24] A. Fukuda, Yo. Takanishi, T. Isozaki, K. Ishikama, and H. Takezoe, *J. Mater. Chem.* **4**, 997 (1994).
- [25] S. Tanaka and M. Yamashita, *Jpn. J. Appl. Phys., Part 1* **38**, L139 (1999).
- [26] R. R. Netz and A. N. Berker, *Phys. Rev. Lett.* **68**, 333 (1992).
- [27] J. S. Smart, *Effective Field Theories of Magnetism* (Saunders, Philadelphia, 1966).
- [28] C. Kittel, *Introduction to Solid State Physics* (Wiley, New York, 1996).
- [29] B. E. Vugmeister and H. Rabitz, *J. Stat. Phys.* **88**, 471 (1997).
- [30] A. G. Anders, S. V. Volotskii, S. V. Startsev, A. Feger, and A. Orendacheva, *Low Temp. Phys.* **21**, 52 (1995).
- [31] A. A. Loginov and Y. V. Pereverzev, *Low Temp. Phys.* **24**, 652 (1998).